Proceedings of the ASME 2018 International Design Engineering Technical Conferences & Computers and Information in Engineering Conference
IDETC/CIE 2018
August 26-29, 2018, Quebec City, Quebec, Canada

DETC2018-85863

FLEXURE-PIVOT OSCILLATOR RESTORING TORQUE NONLINEARITY AND ISOCHRONISM DEFECT

E. Thalmann[*], **M.H. Kahrobaiyan,** **S. Henein**
École Polytechnique Fédérale
de Lausanne (EPFL),
Instant-Lab, Microcity,
CH-2000 Neuchâtel, Switzerland
etienne.thalmann@epfl.ch
mohammad.kahrobaiyan@epfl.ch
simon.henein@epfl.ch

ABSTRACT

Flexure pivot based oscillators can advantageously replace the hairspring and balance wheel, the time base used in mechanical watches, by drastically reducing friction. However, flexure pivots have drawbacks including gravity sensitivity and restoring torque nonlinearity. In previous work, we introduced a novel gravity insensitive flexure pivot (GIFP) to solve the problem of gravity sensitivty, but no analytical formulation for the restoring torque nonlinearity was found. In this paper, we use numerical simulation to find an empirical expression for restoring torque nonlinearity. We use this expression to find an analytical formula for the rotational stiffness of GIFP. This formula gives an explicit relationship between restoring torque nonlinearity and the isochronism of the corresponding harmonic oscillator. The results also apply to the widely used generalized cross-spring pivot.

INTRODUCTION

Mechanical watch oscillators

Classical mechanical watches use a harmonic oscillator consisting of a spiral spring attached to a balance wheel as time base. The balance wheel pivots on jeweled bearings producing significant friction. In order to reduce this friction, flexure pivots [1] [2] have been introduced into watch movements [3], thereby suppressing the need for lubrication, increasing watch autonomy and oscillator quality factor. This last quantity is believed to be the most significant indicator of chronometric performance [4]. In addition to their rotational bearing function, flexure pivots provide an elastic restoring torque which can be used as spring for a harmonic oscillator. In this way, a single monolithically fabricated component can replace the classical balance wheel, spring and bearing.

However, some issues intrinsic to flexure mechanisms limit their application to time bases.

Limitation 1. Gravity sensitivity: spring stiffness can be affected by the orientation of gravity load.

Limitation 2. Restoring torque nonlinearity: spring restoring torque can be a nonlinear function of rotation angle leading to an isochronism defect.

Limitation 3. Limited stroke: stroke of flexure bearings is limited by the yield stress of the material. Limited stroke makes it difficult to maintain and count oscillation using classical watch escapements.

Limitation 4. Parasitic shift: by construction, the kinematics of flexure pivots closely approximate rotational motion around a fixed axis but small translation can occur as angular rotation increases.

[*]Address all correspondence to this author.

Flexure pivot examples

We consider two flexure pivots: the well-known *Generalized Cross-Spring Pivot* (GCSP, see Fig.1) and the new *Gravity-Insensitive Flexure Pivot* (GIFP, see Fig. 2) introduced by the authors in Ref. [5]. The behavior of these flexure pivots can be characterized by a geometric parameter δ, the ratio at which the leaf springs cross [5] [6].

In the case of GCSP, $\delta = d_c/L_c$, where L_c is the length of the leaf springs and d_c is the distance between the mobile end of the springs and the point of intersection of the undeflected springs, see Fig. 1. To a first approximation, the pivot only allows rotation about an axis through this point of intersection [7]. When $\delta \leq 0$, the rotation axis passes through the leaf springs, see Fig. 1(a), this pivot first described by Wittrick [6] is sometimes called *Cross-Spring Pivot* in the literature [7] [8] [9] [10]. When $\delta > 0$, the rotation axis lies outside of the physical spring structure, see Fig. 1(b), this pivot is sometimes called *Remote Center Compliance Pivot* (RCC) [9] or *Leaf-type Isosceles-Trapezoidal Flexural Pivot* (LITF) [11] in the literature. The only configuration considered here is when the flexure beams cross at an angle of 90 degrees.

Figure 2 depicts the GIFP. It consists of a rigid-body (1) attached to the ground (0) by five flexible beams: four bending beams (2), (3), (4) and (5), and a single torsional beam (6). The single degree of freedom is rotation around the torsional beam axis [5]. The geometric parameter is $\delta = d_g/L_g$, where L_g is the length of the bending beams and d_g is the distance between the rotation axis and the mobile end of these beams. Similarly to GCSP, when $\delta \leq 0$, the bending beams cross the rotation axis, see Fig. 2(a), and when $\delta > 0$ the beams do not intersect it, see Fig. 2(b).

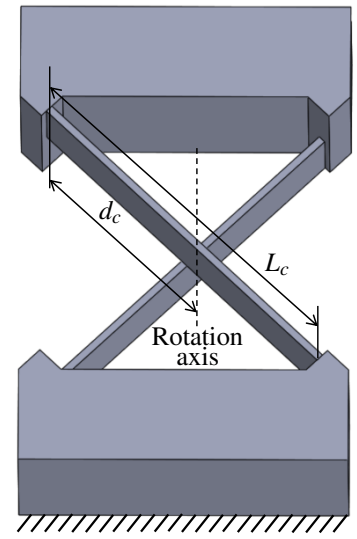

(a) $\delta \leq 0$ (Cross-spring pivot)

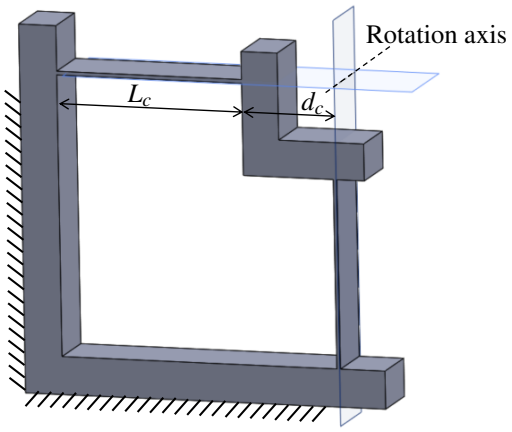

(b) $\delta > 0$ (Remote center compliance pivot)

FIGURE 1: Two configurations of the generalized cross-spring pivot.

Previous results

We addressed limitations 1 and 3 for GCSP and GIFP in Ref. [5], where we derived analytical formulas for gravity sensitivity and stroke then validated them using finite element analysis (FEA). We found special values of the geometric parameter δ which overcome limitations 1 and 3 then showed that for any value of δ, GIFP stiffness variation due to gravity load affects time base precision of order 1 second per day, so acceptable in watchmaking. Limitation 4, parasitic shift of flexure pivot center of rotation, is a well-studied subject, see Refs. [8] and [10], and is already addressed by minimizing gravity sensitivity. Indeed, since gravity sensitivity is caused by the work of gravity load acting along the parasitic shift of the center of gravity, minimizing gravity sensitivity also minimizes parasitic shift.

New results

Limitation 2 has not been well described yet and is the focus of this paper. The analytical formula for restoring torque nonlinearity derived in Ref. [5] is unsatisfactory since it was not validated by FEA simulation. Since this expression is crucial for the design of mechanical time bases, we now use FEA to derive an empirical expression for the nonlinearity of cross beam pivots. Additionally, we extend the analysis to pivots whose springs do not intersect the rotation axis ($\delta > 0$). This is useful for designing systems having rotation axes outside of their physical structure.

Effect of restoring torque nonlinearity on isochronism

The key to chronometric performance is the *isochronism* of its time base stating that oscillation period is independent

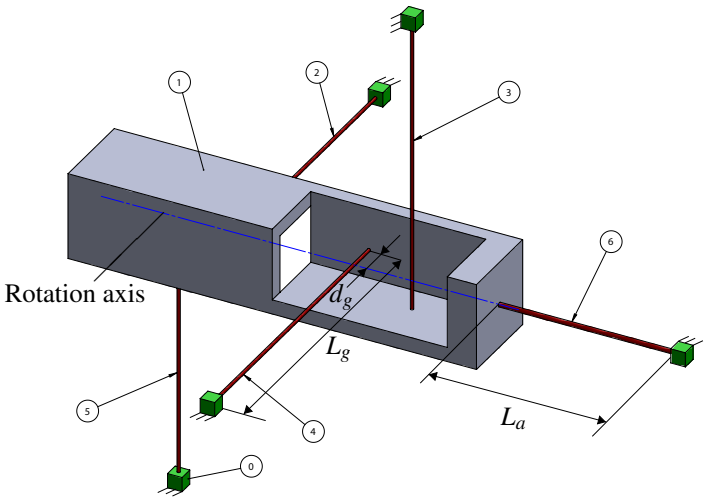

(a) GIFP with $\delta \leq 0$

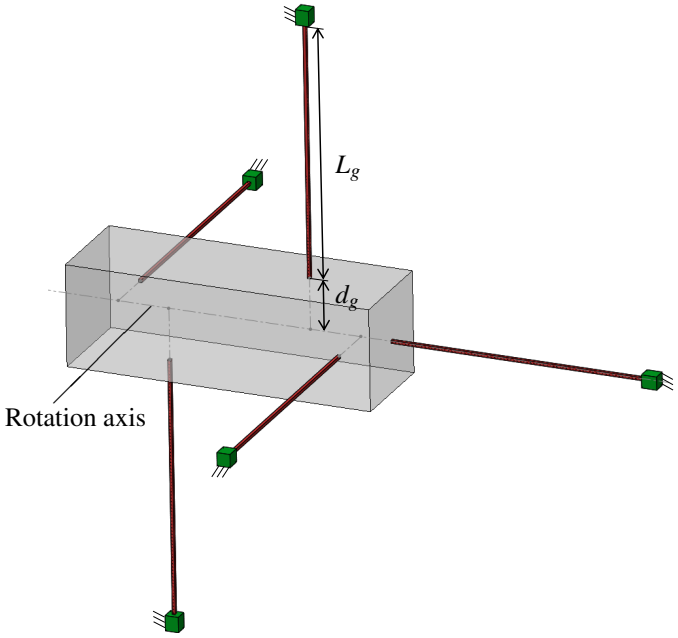

(b) GIFP with $\delta > 0$

FIGURE 2: Two configurations of the gravity-insensitive flexure pivot.

of oscillation amplitude, since this frees the measure of time from variations of maintaining energy [12]. This property was first formulated by Galileo, who incorrectly stated that it applies to pendulum, and first applied by Huygens who designed an isochronous pendulum in 1656. Huygens followed this up with the invention of the spiral spring and balance wheel in 1675, which is theoretically isochronous.

The key to isochronism is Hooke's Law stating that restoring force is a linear function of displacement, since the frequency of an oscillator with mass m and spring stiffness k is then given by $\sqrt{k/m}$, where the amplitude does not appear (in the case of rotational oscillators, this is $\sqrt{k/J}$, where J is moment of inertia). It follows that spring nonlinearity leads to an isochronism defect.

The first flexure pivot used as a mechanical watch time base, a cross-spring pivot oscillator introduced in 2014 [3], uses a special geometry which minimizes the effect of gravity on stiffness [13] and a separate mechanism called *isochronism corrector* to compensate for its nonlinearity. On the other hand, the GIFP oscillator can be made *essentially isochronous* by choosing the correct value of the design parameter δ where the second order term of the rotational stiffness is cancelled ($k_2 = 0$ in Eq. (1)) and gravity sensitivity is of order 10 ppm, see Ref. [5].

For a pivot whose rotational stiffness varies with respect to angular amplitude, we define *relative nonlinearity* to be the relative deviation of the rotational stiffness from the nominal value defined as the limiting value as rotation angle approaches zero [5]. To make this explicit, we consider sufficiently small amplitudes of the pivot when stiffness can be expressed as a power series with even coefficients (due to symmetry) $k = k_0 + k_2\theta^2 + \mathcal{O}(\theta^4)$. In watchmaking applications, this approximation is acceptable for amplitudes where the resulting error on frequency is less than 1 s/day, that is approximately 5 degrees for the most nonlinear RCC pivot considered ($\delta = 1$) and 10 degrees for the most nonlinear cross-spring pivot ($\delta = -0.5$). We then define relative nonlinearity to be

$$\mu = \frac{k_2}{k_0}. \tag{1}$$

We now derive a formula expressing the effect of restoring torque nonlinearity on oscillator accuracy. In mechanical horology, this accuracy is usually expressed as *daily rate*, that is, the gain or loss of the timekeeper expressed in seconds per day. More precisely, given an oscillator with nominal amplitude α_0 and nominal angular frequency ω_0, the daily rate at amplitude α with corresponding frequency ω is defined to be

$$\rho = 86400\,\frac{\omega - \omega_0}{\omega_0}, \tag{2}$$

where 86400 is the number of seconds in one day [14].

Using standard techniques of classical mechanics [15, Eq. 2.3.34] we derive the frequency ω of a non-linear oscillator at amplitude α with relative nonlinearity μ

$$\omega(\alpha) = \omega_0(1 + \frac{3\mu}{8}\alpha^2), \tag{3}$$

where $\omega_0 = \sqrt{k_0/J}$.

The classical horological definition of isochronism considers oscillator rate with respect to oscillator amplitude [12]. We instead use the approach described in Ref. [16], which considers that oscillator rate varies with respect to oscillator energy E. This method has the advantage of holding for 2 degree-of-freedom oscillators whose amplitude is not easy to measure. Using oscillator energy is equivalent to the classical horological definition since, in that case, energy is proportional to the square of oscillator amplitude. Note that the isochronism defect with respect to energy is double that of the equivalent isochronism defect with respect to amplitude since $(1+\varepsilon)^2 \approx 1+2\varepsilon$ for small ε.

Using this method, the relative energy variation with respect to oscillator energy at nominal amplitude E_0 expressed in percentage is defined by

$$E_{\%} = \frac{100\,(E-E_0)}{E_0} = \frac{100\left(\alpha^2-\alpha_0^2\right)}{\alpha_0^2}. \tag{4}$$

Finally, we define the *isochronism defect* σ by dividing the daily rate ρ by the relative energy variation $E_{\%}$. Inserting Eq. (3) into Eq. (2) we obtain

$$\sigma = \frac{\rho}{E_{\%}} = 864\frac{\frac{3}{8}\mu\alpha_0^2}{1+\frac{3}{8}\mu\alpha_0^2}. \tag{5}$$

We arrive at a simpler expression using Taylor series expansion around $\alpha_0^2 = 0$

$$\sigma = 324\mu\alpha_0^2 + \mathscr{O}\left(\alpha_0^4\right). \tag{6}$$

Isochronism is measured experimentally by computing the slope of daily rate σ vs relative energy variation expressed in percentage $E_{\%}$, as illustrated in Fig. 5.

Finite element analysis

We used nonlinear FEA to find the nonlinear torque-angle relationship of flexure pivots having different δ values. For each geometry, 100 incremental displacement values were applied to the mobile part of the pivot and the reaction torque on the fixed frame was measured. When neglecting the effect of the torsional beam of GIFP, the formulas for restoring torque of GIFP and GCSP are identical (see details below), so we only carried out the simulations on a numerical model of GCSP. The simulations were performed using ANSYS®Workbench, Release 19, with shell elements for the flexible blades. The mesh used for the blades consisted of 6 by 100 identical rectangular linear shell elements (shell181). The convergence of this mesh was such that doubling the number of elements led to variations of the restoring torque of less than 0.025% for the greatest displacement simulated, so we consider our results to be robust.

The simulations were carried out for values of δ ranging from -0.5 to 1. Due to symmetry, analysis of pivots with $\delta < -0.5$ reduces to the results presented here with $\delta' = -\delta - 1$. The behavior of the pivots for values of $\delta > 1$ is not investigated due to high stiffness, high nonlinearity and short stroke of these pivots limiting their application. The results obtained should however also be valid in this range.

We validated the finite element model using an analytical model for pivot stiffness. As shown in Ref. [5], the nominal stiffness in the absence of gravity of GIFP pivots is

$$k_0 = k_a + \frac{16EI_g}{L_g}\left(3\delta^2+3\delta+1\right), \tag{7}$$

where E and I_g are Young's modulus and the area moment of inertia of the bending beams and k_a is the torsional stiffness of the torsional beam. We previously found that the stiffness of the torsional beam does not play a major role in the restoring torque nonlinearity of the pivot [5], so we neglected this beam in our analysis. The resulting normalized nominal stiffness was found to be

$$\bar{k}_0 = 3\delta^2+3\delta+1, \tag{8}$$

which is is identical to the normalized nominal stiffness of GCSP, as it corresponds to the normalized nominal stiffness of the cross-spring pivot in Ref. [5, Eq. 9] when $\delta \leq 0$, and to the normalized stiffness of the RCC pivot in Ref. [9, Eq. 5.6] when $\delta > 0$. Figure 3 shows a good match between FEA results and analytical nominal stiffness, validating the finite element model.

RESULTS

The restoring torque nonlinearity is obtained by fitting an odd cubic polynomial to the torque-angle relationship obtained by numerical simulations for chosen values of δ. The relative nonlinearity $\mu = k_2/k_0$ is extracted from the torque-angle relationship $M(\theta) = k_0\theta + k_2\theta^3$ using Eq. (1). The results are shown in Fig. 4. A quadratic curve fits the data well with a coefficient of determination $R^2 = 0.9999$. The resulting empirical expression for stiffness nonlinearity is

$$\mu = -0.08 - 1.00\delta - 1.02\delta^2. \tag{9}$$

Remark: The value $\delta = 0.088$ solves the equation $\mu = 0$ and cancels the nonlinearity.

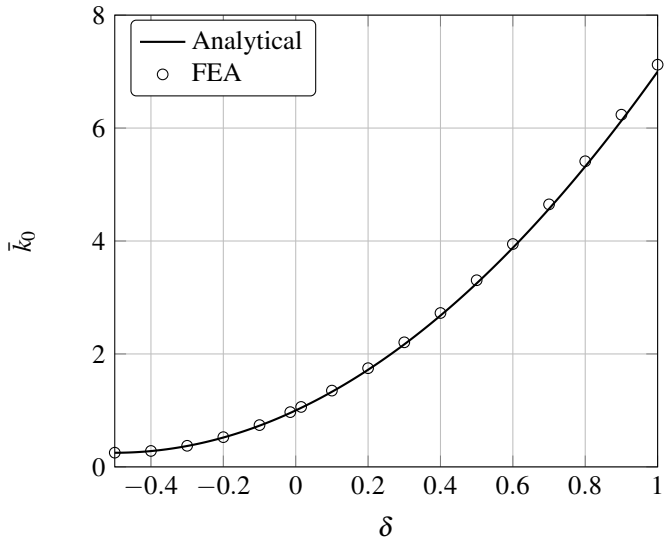

FIGURE 3: Normalized nominal stiffness $\bar{k}_0$ of the GCSP versus geometric parameter δ.

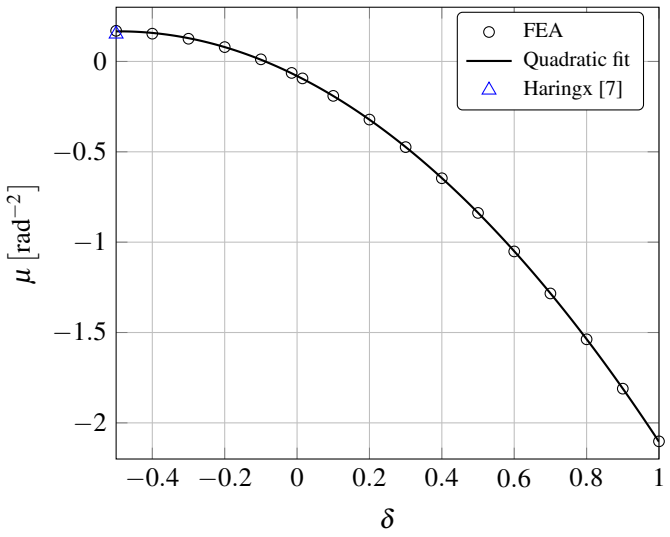

FIGURE 4: relative restoring torque nonlinearity μ of GCSP versus geometric parameter δ.

The analytical solution derived by Haringx in Ref. [7, Eq. 37] for the nonlinear torque-angle relationship of GCSP with $\delta = -0.5$ is plotted on Fig. 4 and matches the FEA results. Note that Haringx's analytical model is limited to the generalized cross-spring pivot with $\delta = -0.5$ since he solved the nonlinear equations using the inherent symmetry which holds only for this configuration.

Since the quadratic curve for the relative nonlinearity fits the data well, we can use it to give a new formula for the stiffness of our pivots. Substituting Eq. (9) into Ref. [5, Eq. 11] which has been validated for describing the effect of normalized external load $\bar{N}$ on the stiffness of GIFP, we obtain the following new formula for the rotational stiffness of GIFP:

$$\begin{aligned} k_g = &\frac{16EI_g}{L_g}\left(3\delta^2+3\delta+1\right)\left[1-\left(0.08+1.00\delta+1.02\delta^2\right)\theta^2\right] \\ &-\frac{EI_g}{12600L_g}\left(9\delta^2+9\delta+11\right)\bar{N}^2+k_a+\mathscr{O}\left(\theta^4\right) \\ &+\mathscr{O}\left(\theta^2\bar{N}^2\right)+\mathscr{O}\left(\bar{N}^4\right). \end{aligned} \tag{10}$$

Similarly, using Ref. [5, Eq. 8], we obtain the following new formula for the rotational stiffness of GCSP:

$$\begin{aligned} k_c = &\frac{8EI_c}{L_c}\left(3\delta^2+3\delta+1\right)\left[1-\left(0.08+1.00\delta+1.02\delta^2\right)\theta^2\right] \\ &+\frac{2EI_c}{15L_c}\left(9\delta^2+9\delta+1\right)\bar{N}\left(\sin\varphi+\cos\varphi\right) \\ &-\frac{EI_c}{6300L_c}\left(9\delta^2+9\delta+11\right)\bar{N}^2+\mathscr{O}\left(\theta^2\bar{N}\right)+\mathscr{O}\left(\theta^4\right)+\mathscr{O}\left(\bar{N}^3\right) \end{aligned} \tag{11}$$

where E, I_c are Young's modulus and the area moment of inertia of the leaf springs and φ is the angle between a normalized external load $\bar{N}$ and the mid-plane of one of the leaf springs in undeflected position.

Figure 5 shows isochronism curves for five chosen values of δ. The isochronism defect is obtained from the slope of the linear curves of daily rate σ vs relative energy variation $E_{\%}$. We can see that the special value $\delta = 0.088$, which cancels the restoring torque nonlinearity in Eq. (9), shows no isochronism defect. Note that the sign of the nonlinearity defines the sign of the isochronism defect.

CONCLUSION AND PERSPECTIVES

In this paper, we derived the stiffness nonlinearity of the generalized cross-spring pivot and the gravity-insensitive flexure pivot.

Mastering the stiffness nonlinearity of a flexure element is a powerful tool, which can produce constant stiffness by minimizing nonlinearity. It can also provide a method for choosing a nonlinearity which can compensate some other unwanted effect. For example, it is known that mechanical escapements introduces an isochronism defect. This defect could be compensated by choosing an oscillator with an isochronism defect of same magnitude but opposite sign, as is the case for pendulum clocks where the intrinsic isochronism defect of the pendulum can be compensated by the escapement [17]. To this end, we showed that we could change the sign and magnitude of the isochronism defect by varying the point at which the springs cross, offering the possibility of cancelling a wide range of defects.

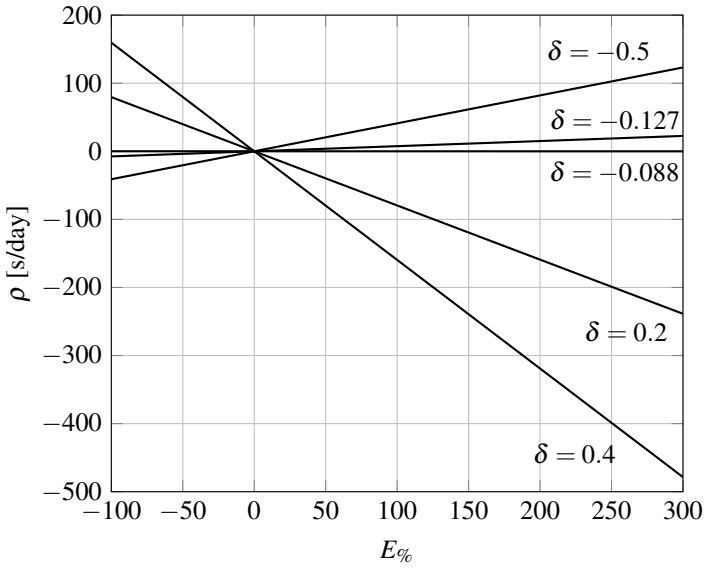

FIGURE 5: Daily rate ρ of GCSP with different values of geometric parameter δ for amplitudes α between 0 deg and 10 deg and nominal amplitude α_0=5 deg.

REFERENCES

[1] Eastman, F. S., 1937. "The Design of Flexure Pivots". *Journal of the Aeronautical Sciences,* ***5***(1), pp. 16–21.

[2] Eastman, F. S., 1935. *Flexure pivots to replace knife edges and ball bearings, an adaptation of beam-column analysis,*. Engineering Experiment Station series. University of Washington, Seattle, USA.

[3] Barrot, F., Dubochet, O., Henein, S., Genequand, P., Giriens, L., Kjelberg, I., Renevey, P., Schwab, P., and Ganny, F., 2014. "Un nouveau régulateur mécanique pour une réserve de marche exceptionnelle". In Actes de la Journée d'Etude de la Société Suisse de Chronométrie, pp. 43–48.

[4] Bateman, D. A. "Vibration theory and clocks". *Horological Journal,* ***120-121***(seven parts July 1977 to January 1978).

[5] Kahrobaiyan, M. H., Thalmann, E., Rubbert, L., Vardi, I., and Henein, S., 2018. "Gravity-Insensitive Flexure Pivot Oscillators". *Journal of Mechanical Design,* ***140***(7), May, pp. 075002–075002–9.

[6] Wittrick, W., 1951. "The properties of crossed flexure pivots, and the influence of the point at which the strips cross". *The Aeronautical Quarterly,* ***2***, pp. 272–292.

[7] Haringx, J. A., 1949. "The cross-spring pivot as a constructional element". *Flow, Turbulence and Combustion,* ***1***(1), Dec., p. 313.

[8] Hongzhe, Z., and Shusheng, B., 2010. "Accuracy characteristics of the generalized cross-spring pivot". *Mechanism and Machine Theory,* ***45***(10), pp. 1434–1448.

[9] Cosandier, F., Henein, S., Richard, M., and Rubbert, L., 2017. *The Art of Flexure Mechanism Design*. EPFL Press, Lausanne, Switzerland.

[10] Marković, K., and Zelenika, S., 2017. "Optimized cross-spring pivot configurations with minimized parasitic shifts and stiffness variations investigated via nonlinear FEA". *Mechanics Based Design of Structures and Machines,* ***45***(3), July, pp. 380–394.

[11] Pei, X., Yu, J., Zong, G., and Bi, S., 2012. "A Family of Butterfly Flexural Joints: Q-LITF Pivots". *Journal of Mechanical Design,* ***134***(12), Nov., p. 121005.

[12] Defossez, L., 1950. *Théorie générale de l'horlogerie*. Chambre suisse de l'horlogerie.

[13] Henein, S., and Kjelberg, I., 2015. Timepiece oscillator, Dec. Patent Number: US9207641B2.

[14] Reymondin, C.-A., Monnier, G., Jeanneret, D., and Pelaratti, U., 1999. *The Theory of Horology*. Swiss Federation of Technical Colleges.

[15] Nayfeh, A., and Mook, D., 1979. *Nonlinear Oscillations*. Wiley, Jan.

[16] Vardi, I., Rubbert, L., Bitterli, R., Ferrier, N., Kahrobaiyan, M., Nussbaumer, B., and Henein, S., 2018. "Theory and design of spherical oscillator mechanisms". *Precision Engineering,* ***51***, Jan., pp. 499–513.

[17] Rawlings, A. L., 1993. *The Science of Clocks & Watches*, third and revised edition edition ed. British Horological Institute, Upton, UK.